Neuron, Vol. 35, 575–587, August 1, 2002, Copyright ©2002 by Cell Press

Delayed Striate Cortical Activation during Spatial Attention

Toemme Noesselt,[1,5] Steve A. Hillyard,[3] Marty G. Woldorff,[4] Ariel Schoenfeld,[1] Tilman Hagner,[1] Lutz Jäncke,[2] Claus Tempelmann,[1] Hermann Hinrichs,[1] and Hans-Jochen Heinze[1]

[1]Department of Neurology II
[2]Institute of General Psychology
Otto-von-Guericke-University
39120 Magdeburg
Germany
[3]Department of Neurosciences
University of California, San Diego
La Jolla, California 92093
[4]Center for Cognitive Neuroscience and
Department of Psychological and Brain Sciences
Duke University
Durham, North Carolina 27708

Summary

Recordings of event-related potentials (ERPs) and event-related magnetic fields (ERMFs) were combined with functional magnetic resonance imaging (fMRI) to study visual cortical activity in humans during spatial attention. While subjects attended selectively to stimulus arrays in one visual field, fMRI revealed stimulus-related activations in the contralateral primary visual cortex and in multiple extrastriate areas. ERP and ERMF recordings showed that attention did not affect the initial evoked response at 60–90 ms poststimulus that was localized to primary cortex, but a similarly localized late response at 140–250 ms was enhanced to attended stimuli. These findings provide evidence that the primary visual cortex participates in the selective processing of attended stimuli by means of delayed feedback from higher visual-cortical areas.

Introduction

Visual attention may be directed voluntarily to a selected region of the visual field in order to facilitate the perceptual analysis of objects and events at that spatial location. A key unresolved question about the brain systems subserving visual-spatial attention concerns the level of the visual pathways at which incoming information is modulated (i.e., either enhanced or suppressed) by attention. Numerous neurophysiological studies in animals and neuroimaging studies in humans have shown that attended inputs are modulated in multiple extrastriate cortical regions including higher areas of both the dorsal and ventral processing streams (reviewed in Desimone, 1998; Maunsell and McAdams, 2000; Martinez et al., 2001). The role of the primary visual cortex (area V1) in attentional selection, however, continues to be a topic of controversy (Posner and Gilbert, 1999; Sengpiel and Huebener, 1999).

[5]Correspondence: toemme@neuro2.med.uni-magdeburg.de

Until recently there was little evidence to suggest that visual information processing in area V1 could be modulated by spatial attention. A study in monkeys by Motter (1993) had found that evoked activity in some V1 neurons could be either increased or decreased by directing the animal's attention to the stimulus location. However, numerous investigations in humans using electrophysiological and neuroimaging techniques failed to find evidence for any modification of neural activity in V1 by spatial attention (Heinze et al., 1994; Clark and Hillyard, 1996; Gratton, 1997; Mangun et al., 1997; Wijers et al., 1997; Woldorff et al., 1997; Lange et al., 1998). These findings suggested that the visual pathways in V1 may only subserve passive sensory transmission and are not subject to cognitive control under a wide range of attentional tasks.

During the past few years, however, several studies in monkeys have affirmed Motter's (1993) earlier finding that neural activity in V1 may be modified by attention under certain circumstances, particularly in discrimination tasks when several competing stimuli are present in the visual field (Roelfsema et al., 1998; Vidyasagar, 1998; Ito and Gilbert, 1999; McAdams and Maunsell, 1999). Interestingly, the observed increases in neural discharge in V1 related to attention generally occurred at fairly long latencies (80–100 ms after stimulus onset, whereas initial V1 activity in the monkey begins at 40–50 ms), suggesting that attentional influences on V1 neurons may be controlled by delayed feedback projections from higher visual areas (Vidyasagar, 1999). This feedback hypothesis was strongly supported by Mehta et al.'s (2000) intracerebral recordings of event-related potentials (ERPs) from monkeys, which showed that attentional modulations of the visual ERP were larger and occurred earlier in area V4 than in lower-tier areas V2 and V1. These findings were consistent with a feedback mechanism whereby visual information was first enhanced by attention in higher cortical areas and then projected back to lower areas, perhaps improving the perceptual salience and figure-ground segregation of stimuli at attended locations (Lamme and Spekreijse, 2000).

Evidence that neural activity in area V1 may be strongly affected by spatial attention in humans has come from recent fMRI studies (Tootell et al., 1998; Brefczynski and DeYoe, 1999; Gandhi et al., 1999; Martinez et al., 1999; Somers et al., 1999). In these studies, two or more sequences of stimuli were presented concurrently to different locations in the visual fields, and subjects were required to discriminate events in one sequence at a time. The general finding was an increase in neural activity in circumscribed zones of area V1 corresponding to the retinotopic projection of the attended stimulus location. Given the low temporal resolution of fMRI, however, it was not clear whether these topographically organized increases in neural activity were the result of direct modulation of early sensory-evoked activity in V1, a delayed modulation of activity in V1 due to feedback from higher visual areas, or a sustained increase in baseline neural activity associated with the

spatial focusing of attention (Luck et al., 1997; Kastner et al., 1999; Ress et al., 2000).

These alternative mechanisms were investigated in a recent study (Martinez et al., 1999) that combined ERP recordings with fMRI in order to examine the time course of neural activity enhanced by attention in different cortical areas. In this study, subjects were required to discriminate a central letter target from surrounding distractors in stimulus arrays that were presented in random order to the left and right visual fields. The fMRI data showed attention-related increases in neural activity in retinotopic areas V1, V2, V3/VP, and V4v in the hemisphere contralateral to the attended visual field. ERP recordings obtained in a separate session, however, showed no evidence of attentional modulation of the early "C1" component (onset at 50 ms) that is considered to be the initial evoked response in primary visual (striate) cortex. Accordingly, it was suggested that the increased activity in area V1 seen with fMRI might be the result of delayed processing of enhanced feedback signals to V1 from higher visual areas. Dipole modeling of the neural sources of these ERPs was consistent with a delayed attention effect in area V1 (Martinez et al., 2001), but it was difficult to distinguish V1 activity from concurrently active sources in neighboring extrastriate cortex in these ERP recordings.

The present study employed recordings of both magnetic and electrical brain responses in conjunction with fMRI in order to clarify the participation of area V1 in spatial selective attention. On each trial, subjects were shown an attention-directing cue, which was followed after a short interval by a rapidly presented sequence of bilateral stimuli, one side of which was to be attended (Figure 1). The overlapping BOLD responses to the cue and to the bilateral stimuli were differentiated by a linear deconvolution technique (Dale, 1999; Josephs and Henson, 1999; Burock and Dale, 2000; Hinrichs et al., 2000), and attention-related modulations were localized with respect to retinotopically mapped borders of striate and extrastriate visual areas (Sereno et al., 1995). Colocalization of the hemodynamic and electromagnetic attention effects obtained in separate sessions in the same subjects yielded information about the time course of striate and extrastriate activations. The combined recording of ERPs and event-related magnetic fields (ERMFs) allowed detection of both tangential and radially oriented neural sources within the different cortical areas. Using these techniques, the aim was to determine whether attention-related BOLD effects in V1 reflect the anticipatory cueing of attention or the subsequent processing of the task stimuli, and in the latter case, whether a delayed attentional modulation in area V1 could be observed directly in the electrical and/or magnetic brain recordings.

Results

Behavioral Results

There were no significant differences in target discrimination accuracy between the MEG and fMRI sessions ($F(1,5) = 0.667$; $p > 0.44$). Over both sessions, the mean hit rates (for discriminating inverted versus upright "T"s) at attended locations in the right and left hemifields were 84.0% and 84.6% (SD = 7.7% and 7.1%), respectively, with no significant hemifield difference ($F(1,14) = 0.11$; $p > 0.75$). The corresponding mean d' scores for the left and right hemifields were 2.33 and 2.47. In the neutral condition (no discrimination required), the mean rate of correct responding was 88.1% (SD = 4.7%).

fMRI

Selective attention effects in the six subjects participating in the fMRI experiment were first examined across trial blocks that included both cue- and stimulus-related activity within each trial. In this analysis, the attend-left and attend-right conditions were compared using SPM99 (Wellcome Department of Cognitive Neurology, London, UK). Significant MR signal increases were found in several posterior cortical regions of the hemisphere contralateral to the attended visual field, including the calcarine fissure, lingual and fusiform gyri, middle and inferior occipital gyri, transverse occipital sulcus, and middle and inferior temporal gyri (Figure 2A; Table 1).

The second phase of the analysis separated the overlapping hemodynamic responses associated with the attention-directing cue and the task stimuli, respectively, using a linear deconvolution procedure (Dale, 1999; Hinrichs et al., 2000). Separate statistical analyses of the cue- and stimulus-related BOLD signals were carried out for those voxels that showed significant effects in the blocked design comparison. The cue- and stimulus-related attention effects showed overlapping cortical distributions, with the latter being more spatially extensive and consistent across subjects (Figures 2B and 2C; Table 1). In particular, attention-related activity in the calcarine area was much more prominent in association with the task stimuli than in response to the attention-directing cue.

To localize these attention-related patterns of activity to specific visual areas, significant activations were projected onto flattened representations of each individual's retinotopically mapped visual cortex (Figure 2D). Cue-related attention effects were more evident in higher visual areas, while stimulus-related effects formed a chain of activations in retinotopic areas V1, V2v, VP, and V4v at cortical locations representing the attended stimulus position in the contralateral upper visual field. Stimulus-related activations were also seen in the fusiform gyrus anterior to area V4v, in the upper field map of area V3a, and in the middle occipital gyrus/transverse occipital sulcus anterior to area V3a. The enhancement of stimulus-related activity in area V1 contralateral to the attended visual field was consistently observed in all subjects (Figure 3A). This contralateral enhancement of neural activity in V1 was also evident when the attend-left and attend-right conditions were contrasted with the neutral condition (Figure 3B).

To quantify the degree of lateralization of the attention-related neural activity in the different areas, the stimulus-related BOLD signals from the hemisphere contralateral to the attended visual field were compared with those from the ipsilateral hemisphere and with those obtained in the neutral condition (Figure 3C). For each area, a laterality index was calculated as the ratio of BOLD signal amplitudes over 6–16 s after stimulus

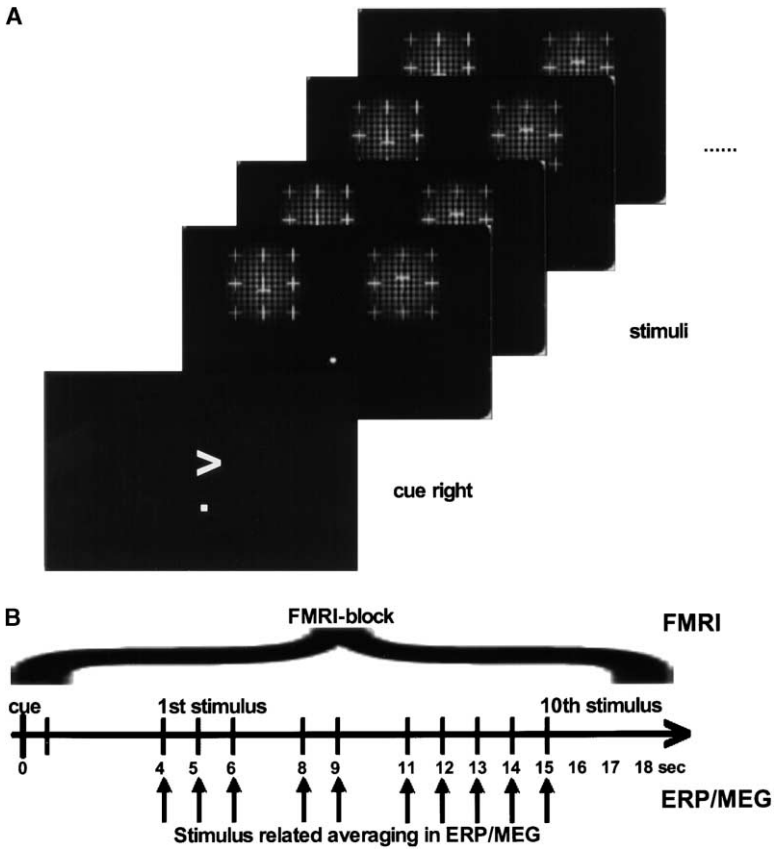

Figure 1. Stimuli and Task Design

(A) The arrow cue directed subjects to attend to the stimulus array in either the right or left visual field on each trial.

(B) The fMRI analyses included attend-left versus attend-right comparisons of activity across entire trials (blocked analysis) as well as separate comparisons of cue-related and stimulus-related activity separated by deconvolution. ERPs and ERMFs were recorded in response to the individual task stimuli and averaged separately according to attend-left, attend-right, and neutral conditions.

onset for both the attended contralateral/ipsilateral and attended contralateral/neutral comparisons. In both cases, the activity was significantly higher in the contralateral hemisphere in most visual-cortical areas (Figure 3D), indicating a consistent lateralization of attention-related neural activity to the hemisphere contralateral to the attended visual field. This lateralization provides strong evidence that the neural activity in the attend left/right versus neutral comparisons is associated with spatial-selective attention and not with nonspecific aspects of the task such as difficulty differences between the attend and neutral conditions.

ERP Recordings

The ERP waveforms of the nine subjects participating in the concurrent ERP and ERMF recordings included an initial C1 component (onset at ~60 ms, peak at 90–95 ms) having a midline parietal distribution, followed by a P1 wave (onset at about 70 ms, peak at 110–120 ms) that was maximal over lateral occipito-temporal sites (Figure 4A). Also evident were an occipito-parietal N1 (onset at ~140 ms, peak at 160–170 ms) and a broadly distributed P2 (onset at ~200 ms, peak at 220–230 ms).

As in previous studies (e.g., Heinze et al. 1994), the effects of spatial attention on ERPs were evaluated by comparing component amplitudes and distributions in attend-left versus attend-right conditions. Confirming previous reports, the C1 (measured at 60–90 ms at site Pz) was not affected by the direction of attention ($F(1,8) = 0.3$; $p > 0.5$). The earliest effect of attention was an enlarged P1 positivity distributed more laterally at occipito-temporal sites contralateral to the attended visual field (for mean amplitude 90–120 ms at sites PO7/PO8, hemisphere x attended-side interaction, $F(1,8) = 25.6$, $p < 0.001$). The earlier positivity in the 50–80 ms range did not reach significance ($F(1,8) = 3.30$; $p > 0.1$). A later positivity elicited between 150–250 ms at lateral occipito-temporal sites also was larger over the hemisphere contralateral to the attended visual field (for mean amplitude 180–220 ms at sites PO7/PO8 and PO3/PO4, hemisphere x attended-side interaction, $F(1,8) = 5.50$, $p < 0.05$).

The scalp distribution of the C1 component at 80 ms was highly similar for attend-left and attend-right conditions (Figure 4B) with a negative amplitude maximum at midline parietal sites. At lateral occipital sites, the initial phase of the P1 positivity was also evident at 80 ms. The neural sources of C1 were estimated by fitting a single dipole to its grand average voltage distribution during the interval 67–83 ms using the CURRY 4.0 analysis program based on a realistic-head boundary-element model. For both attend-right and attend-left conditions, the best-fit C1 dipoles were situated in the region of the calcarine fissure (Figure 4E) with Talairach coordinates of 3, −74, 20 and 1, −76, 15, respectively; the goodness of fit (GOF) of these dipole solutions (proportion of scalp variance accounted for) was 90% and 94% for attend-right and attend-left, respectively. The sources of the early P1 attention effect during the interval 91–106 ms were estimated by fitting a pair of bilaterally symmetrical dipoles to the grand average attend-right minus attend-left difference distribution (Figure 4C). A dipole

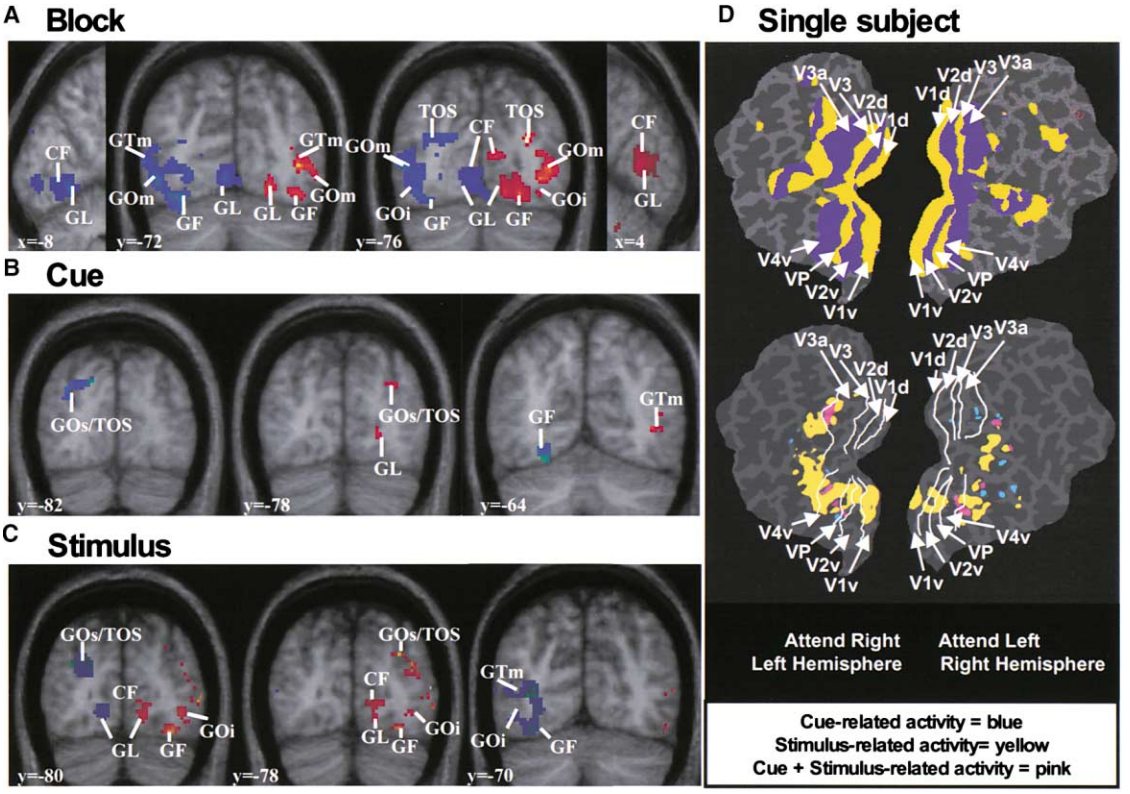

Figure 2. Effects of Attention on fMRI Signals

(A–C) Attention-related fMRI modulations averaged over all subjects and superimposed upon group-average brain sections. Pixels shown in red had significantly larger BOLD signals during attend-left than attend-right conditions, and pixels shown in blue had the reverse. (A) Attend-left versus attend-right comparisons across entire stimulus blocks. (B and C) The same comparisons for cue- and stimulus-related BOLD signals, respectively, separated by deconvolution. Significance criterion was $p < 0.05$, corrected for spatial extent. Abbreviations: CF, calcarine fissure; GL, lingual gyrus; GF, fusiform gyrus; GOm, middle occipital gyrus; GOi, inferior occipital gyrus; GOs/TOS, superior occipital gyrus/transverse occipital sulcus; GTm, middle temporal gyrus; GTi, inferior temporal gyrus.

(D) Top: field sign map of retinotopically organized visual areas in a single subject. Bottom: attention-related fMRI activity superimposed on flattened cortical representations of left and right hemispheres in a single subject. Sulcal cortex is shown in dark gray, gyral in light gray. White lines on activation maps are boundaries of early visual areas traced from the field sign maps. Cue-related activations are shown in blue, stimulus-related activations in yellow, and joint cue plus stimulus activations in pink. The left hemisphere activation map shows areas with greater BOLD signals for attend-right than attend-left conditions, and the right hemisphere activation map shows the reverse ($p < 0.05$, corrected for multiple comparisons).

pair in lateral extrastriate cortex (coordinates −39, −74, 4 and 32, −75, 6) accounted for this early attention effect with GOF = 94% (Figure 4E). The difference map of the late attention effect (Figure 4D) was fit over 201–224 ms with a symmetrical dipole pair situated more dorsally in lateral extrastriate cortex (coordinates −34, −79, 15 and 26, −80, 16) with GOF = 95% (Figure 4E). Note that the estimated dipole locations for the C1 were close to the fMRI activations in the calcarine/V1 area, while the estimated locations of the early P1 and late effect ERP dipoles were close to fMRI activations in the middle and superior occipital gyri, respectively (see Table 1).

ERMF Recordings

The ERMF waveforms were characterized by a prominent M1 component (onset at ~60 ms, peak at 90–100 ms), which, like the electrical C1 component, was not affected by manipulations of attention (Figure 5A). The M1 had a strong dipolar field distribution centered at the midline (Figure 5B) that was well fit in the interval 75–91 ms by dipoles in calcarine cortex (coordinates 4, −81, 8 and 5, −78, 7) with GOF = 94% and 96% (for attend-right and attend-left, respectively; Figure 5E). For the M1 component in the 60–90 ms range, the attended-side x hemisphere interaction did not approach significance for the attend-right versus attend-left comparison ($F(1,8) < 0.1$, $p > 0.9$).

A small attention effect was observed in the ERMF at around 100 ms that may correspond to the electrical P1 effect. The attend-right minus attend-left difference field at 100 ms (Figure 5C) could be modeled by a pair of dipoles in lateral extrastriate cortex (coordinates −31, −81, 11 and 24, −81, 12) with GOF = 91% (Figure 5E). This attentional modulation did not reach statistical significance, however, for any sensor sites.

A more substantial ERMF attention effect was seen in the 140–250 ms range (Figure 5A, late effect). This attention effect was significant at the posterior field

Table 1. Brain Regions Showing Significant Attention-Related Modulations of the BOLD Response

Group Averages					Number of Subjects Showing Effect (n = 6)		
Area	x	y	z	z value	Block	Cue	Stimulus
Attention right minus left							
CF	−8	−76	6	2.01*	6	3	6
GL	−8	−70	0	3.24**	6	5	5
GF	−32	−70	−14	4.06**	6	4	6
GOm	−48	−74	9	3.69**	5	6	5
GOi/GTi	−46	−68	−8	4.47**	5	3	5
GOm/GTm	−56	−74	9	3.35**	5	4	6
TOS/GOS	−26	−76	28	4.10**	6	5	4
Attention left minus right							
CF	8	−73	15	3.61**	6	2	6
GL	14	−74	−3	3.66**	5	3	5
GF	20	−78	−5	4.45**	5	4	6
GOi	40	−78	2	4.67**	5	2	6
GOi/GTi	40	−68	−8	4.04**	6	2	5
GOm/GTm	40	−68	7	4.70**	5	2	6
TOS/GOS	28	−75	22	4.69	6	3	5

Left: Talairach coordinates and z scores for the group analysis (n = 6); *$p < 0.02$, **$p < 0.001$, corrected for spatial extent. Right: number of subjects showing attentional modulation in the block design and, after deconvolution, in the cue- and stimulus-related activations.

maxima (attended-side x hemisphere interaction, $F(1,8) = 10.35$, $p < 0.012$). The attend-right minus attend-left difference field corresponding to this effect (Figure 5D) could be accounted for by two dipoles in the interval 189–224 ms, one situated in calcarine cortex (coordinates 0, −83, 11) and the other in right temporo-parietal cortex (coordinates 47, −30, 13) with GOF = 93% (Figure 5E).

The late ERMF attention effect seen in the attend-right minus attend-left difference field (Figure 5D) was quite weak. In contrast, the difference maps for the attend-left minus neutral and attend-right minus neutral differences showed higher field power and appeared highly similar to one another (Figures 6A and 6B). This suggests that a good deal of attention-related neural activity may have been subtracted out in the late attend-left minus attend-right difference. Further analysis of the attend-left minus neutral and attend-right minus neutral difference fields supports this interpretation. For the M1 time range (60–90 ms), neither of the two comparisons reached significance (attend left-neutral comparison: $F(1,8) = 2.1$, $p > 0.05$; attend right-neutral: $F(1,8) = 3.6$, $p > 0.05$). For the late effect at 189–224 ms, however, both of these comparisons were highly significant, reflecting larger ERMF responses in attend versus neutral conditions: for sensors at the posterior field maxima, condition x hemisphere interaction $F(1,8) = 79.96$, $p < 0.0001$ for attend-left versus neutral, and $F(1,8) = 24.06$, $p < 0.0012$, for attend-right versus neutral.

These attention-related difference fields developed at around 140–150 ms and reached a maximum strength at 210–230 ms (Figures 6A and 6B). Source modeling indicated that these attend-left minus neutral and attend-right minus neutral difference fields could both be accounted for by three dipolar sources in the interval 189–224 ms with GOFs of 92% and 93%, respectively. These sources were located in midline occipital (coordinates −3, −78, 11 for attend-left minus neutral and −3, −83, 5 for attend-right minus neutral), left central (coordinates −38, −25, 56 and −37, −16, 49), and right central (coordinates 23, −17, 59 and 23, −18, 60) areas. Projection of the occipital dipoles onto anatomical sections (Figure 6C) shows them to be situated in calcarine cortex with the same orientation but opposite direction as the dipole fit to the initial M1 component. The similarity in location and orientation of the occipital dipoles accounting for the attend-left minus neutral and attend-right minus neutral difference fields explains why this midline source was largely subtracted out in the attend-right minus attend-left difference field.

The calcarine sources that were active in the interval 150–230 ms during attend-left and attend-right conditions were consistently observed in most individual subjects (Figures 7A–7C). In seven of the nine subjects, the attend-left minus neutral and attend-right minus neutral difference fields could be accounted for by a model having dipoles in calcarine, left central, and right temporal areas with GOFs averaging 89% (range 82%–95%). In each of these subjects, the dipoles fit to the late attend-left and attend-right minus neutral difference fields were in close proximity to the dipole accounting for the early M1 component but had an opposite orientation.

Two additional tests were carried out to confirm the localization of the dipolar source for the late attention effect to the calcarine/V1 region. In the first, dipoles were seeded to the maxima of the fMRI activations in area V1 in the attend-right versus neutral and attend-left versus neutral contrasts for the individual subjects shown in Figure 3B; these V1 dipoles accounted for the late attention effect in the MEG over 200–220 ms better than did dipoles seeded to corresponding fMRI activations in the lingual or fusiform gyri in every subject (mean values are shown in Figure 7D). In the second test, a distributed source model (LORETA) was applied to the EMRF distributions of the attend-left minus neutral and attend-right minus neutral differences over 200–220 ms. The resulting current density distributions (Figure 7E) indicate a tight clustering of sources for the late effect in the calcarine region that closely matches the location of the ECD solutions.

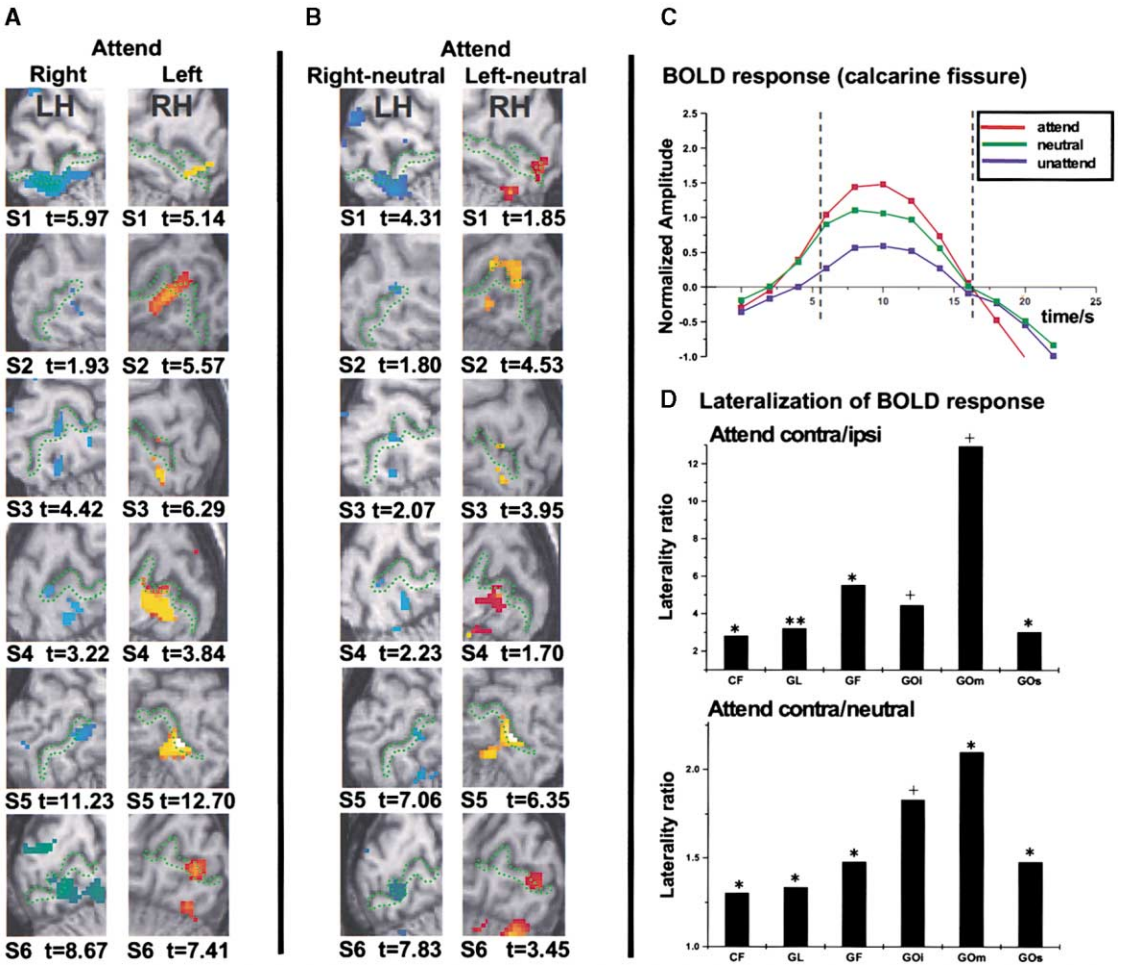

Figure 3. Stimulus-Related Attentional fMRI Modulations in the Calcarine Cortex/Area V1 in Six Individual Subjects

(A and B) Dotted green lines outline the boundaries of area V1v as determined for each subject/hemisphere by retinotopic mapping. Significance levels for local maxima in V1: $t > 1.65$, equivalent to $p < 0.05$, uncorrected; $t > 3.1$, equivalent to $p < 0.001$, uncorrected; $t > 4.65$, equivalent to $p < 0.05$, corrected for multiple comparisons. (A) Left hemisphere activations (blue) represent greater BOLD signals in attend-right than attend-left condition, and right hemisphere activations (yellow to red) represent the reverse. (B) Left hemisphere activations (blue) represent greater BOLD signals in attend-right than neutral condition, and right hemisphere activations (yellow to red) represent greater BOLD signals in attend-left than neutral condition.

(C) Time course of BOLD responses following stimulus onset (time zero on abscissa) in area V1 in hemisphere contralateral to the attended visual field, ipsilateral to the attended field, and under neutral conditions, averaged over all subjects.

(D) Laterality ratios of BOLD response amplitudes in hemisphere contralateral to attended field versus ipsilateral to attended field and versus neutral condition, averaged over all subjects. *$p < 0.05$; **$p < 0.01$; $^{+}p < 0.1$ (repeated measures ANOVA).

Discussion

The present results provide combined electromagnetic and hemodynamic evidence that the primary visual cortex (area V1) plays a role in visual spatial attention that involves receiving delayed feedback signals from higher cortical areas. Whereas the initial response evoked at 60–90 ms that was localized to calcarine cortex by dipole modeling remained unaffected by attention, longer latency activity in the 140–250 ms range having an identical localization was found to be strongly modulated by attention to the task stimuli. This late attention effect observed in the ERMF was also colocalized with a hemodynamic attention effect revealed by fMRI and shown by retinotopic mapping to be situated in area V1 of the hemisphere contralateral to the attended visual field. A deconvolution procedure indicated that these attention-related increases in the BOLD signal in V1 were closely time-locked to presentations of the task stimuli. Together, these findings support the hypothesis that spatially directed attention produces a delayed processing of task-relevant stimuli in primary visual cortex.

The fMRI findings reported here are in line with previous reports that directing attention to a location away from the midline produces an increase in neural activity in multiple areas of the visual cortex of the contralateral hemisphere, including the retinotopic areas V1, V2, V3/VP, V3a, and V4, as well as higher areas belonging to both the dorsal and ventral processing streams (see Introduction). The present experiment separated fMRI activations linked with attentional orienting to the cue from those associated with processing of the task stim-

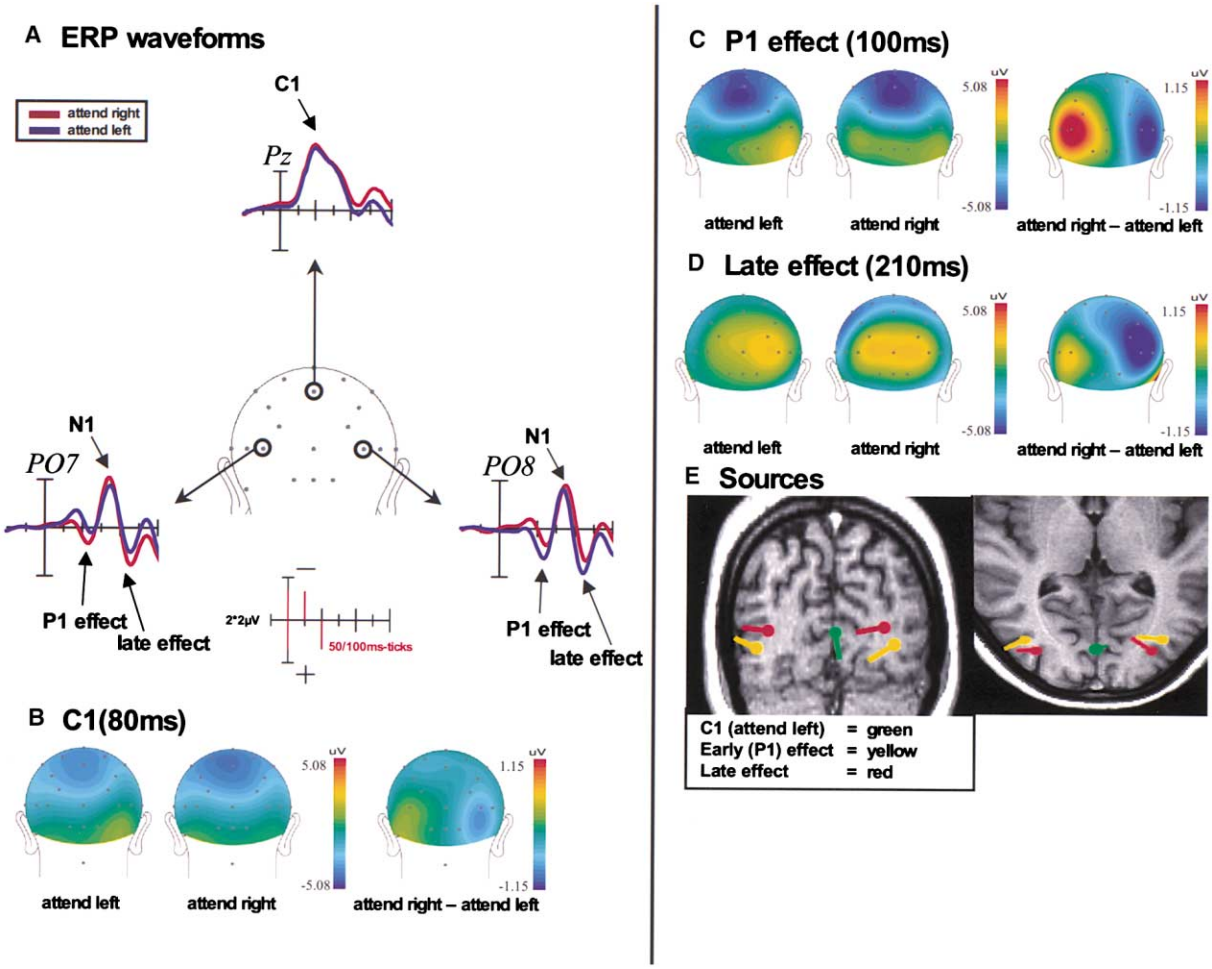

Figure 4. Effects of Attention on ERPs

(A) Grand average ERPs to bilateral task stimuli recorded from midline parietal (Pz) and lateral occipital (PO7/PO8) sites under attend-left and attend right-conditions.

(B–D) Grand average voltage distributions and sources of ERPs. (B) Topography of the C1 component at 80 ms under attend-left and attend-right conditions and the subtracted difference topography. (C) Topography of the early P1 attention effect at 100 ms. (D) Topography of the late attention effect at 210 ms.

(E) Best-fit dipolar sources for the C1 component at 67–83 ms (only attend-left condition is shown, attend-right condition was virtually identical), the early P1 attention effect at 91–106 ms (attend-right minus attend-left difference), and late attention effect at 205–224 ms (attend-right minus attend-left difference). These dipoles were fit to the grand average ERP distributions and projected onto anatomical MRI sections from a single subject.

uli using a deconvolution procedure (Hinrichs et al., 2000). It was found that stimulus-related activity was more pronounced in the lower-level retinotopic visual areas, and in particular, neural activity in the contralateral area V1 was consistently enhanced in response to the task stimuli in every subject. This strong participation of V1 in the selective processing of the attended stimuli may be a consequence of the demanding perceptual discrimination of target information that was required.

Despite this clear fMRI evidence for V1 activity linked to processing the task stimuli, the earliest evoked electrical (C1) and magnetic (M1) responses elicited by those stimuli (at 60–90 ms), which were localized by dipole modeling to calcarine cortex, did not show significant modulation as a function of direction of attention. This lack of sensitivity of the C1 to attentional manipulations is in accordance with previous studies (see Introduction). Several lines of evidence suggest that the C1/M1 components originate from primary visual cortex, including their short latency, calcarine localization, and retinotopic polarity inversion corresponding to the mapping of the upper and lower visual fields onto area V1 within the calcarine cortex (Clark et al., 1995; Aine et al., 1995, 1996; DiRusso et al., 2002). Thus, the present study adds to the evidence that the initial stimulus-evoked activity in area V1 is not influenced by spatial attention.

The earliest ERP modulation produced by attention to the present bilateral stimuli was an enhanced P1 positivity in the range 80–130 ms over the occipital scalp contralateral to the attended visual field. This lateralized P1 effect replicates many previous findings using both

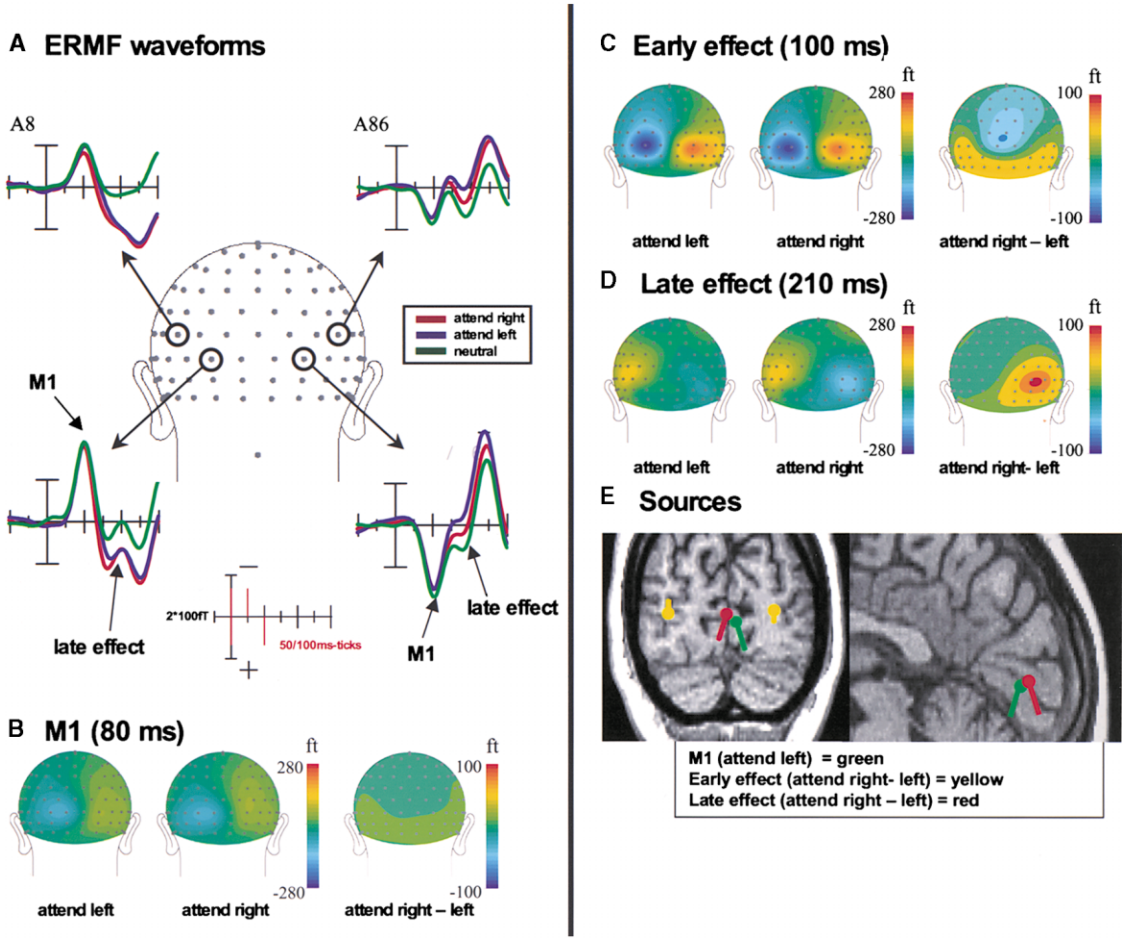

Figure 5. Effects of Attention on ERMFs

(A) Grand average ERMF waveforms to bilateral task stimuli recorded from four posterior sensor sites under the three task conditions. (B–E) Grand average ERMF distributions across magnetometers and modeled dipolar sources: scales in femtotesla (ft). (B) Field topography of the M1 component at 80 ms under the attend-left and attend-right conditions and the subtracted difference topography. (C) Topography of nonsignificant early attention effect at 100 ms. (D) Topography of late attention effect at 210 ms. (E) Best-fit dipolar sources for the M1 (75–91 ms, only attend-left condition shown; attend-right and neutral conditions were found to be virtually identical), early attention effect (87–106 ms, attend-right minus attend-left difference field), and late attention effect (calcarine dipole at 189–224 ms, attend-right minus attend-left difference field). Dipoles were derived from grand average ERMF distributions and projected onto anatomical sections from a single subject.

bilateral (Heinze et al., 1990, 1994; Luck et al., 1990; Mangun et al., 1997; Woldorff et al., 1997) and unilateral (reviewed in Hillyard and Anllo-Vento, 1998) stimuli. All of these studies found the source of the attentionally enhanced P1 wave to be localized to lateral extrastriate cortex, with neural generators in ventral-fusiform and/or mid-occipital regions (Martinez et al., 2001). This early P1 attention effect seen in the ERPs only produced a weak signature in the present MEG recordings, however, probably because its dipolar source had a primarily radial orientation.

Different patterns of longer latency attention effects were detected by the electrical and magnetic recordings. A contralateral positivity in the 150–250 ms range was observed in the ERP recordings, the sources of which were localized by dipole modeling to extrastriate areas (region of the superior occipital gyrus) slightly above the sources calculated for the earlier P1 effect. Those strong extrastriate neural generators might have masked a possible striate source. This lateral occipital activity was not evident in the MEG recordings, probably because its generators also had a primarily radial orientation. The MEG recordings, on the other hand, revealed an attention effect in the 150–250 ms range in the attend-left minus attend-right comparison that was localized to sources in the calcarine cortex and in the right temporo-parietal area. The calcarine source was found to be much stronger in the attend-left and attend-right minus neutral comparisons, most likely because the contralateral amplitude increases were arising from calcarine dipoles in the right and left hemispheres that were adjacent (i.e., near the midline) and similarly oriented and thus were largely cancelled out in the attend-left minus attend-right comparison. Based on its colocalization with the increased stimulus-related BOLD signal in area V1 contralateral to the attended visual field, we propose

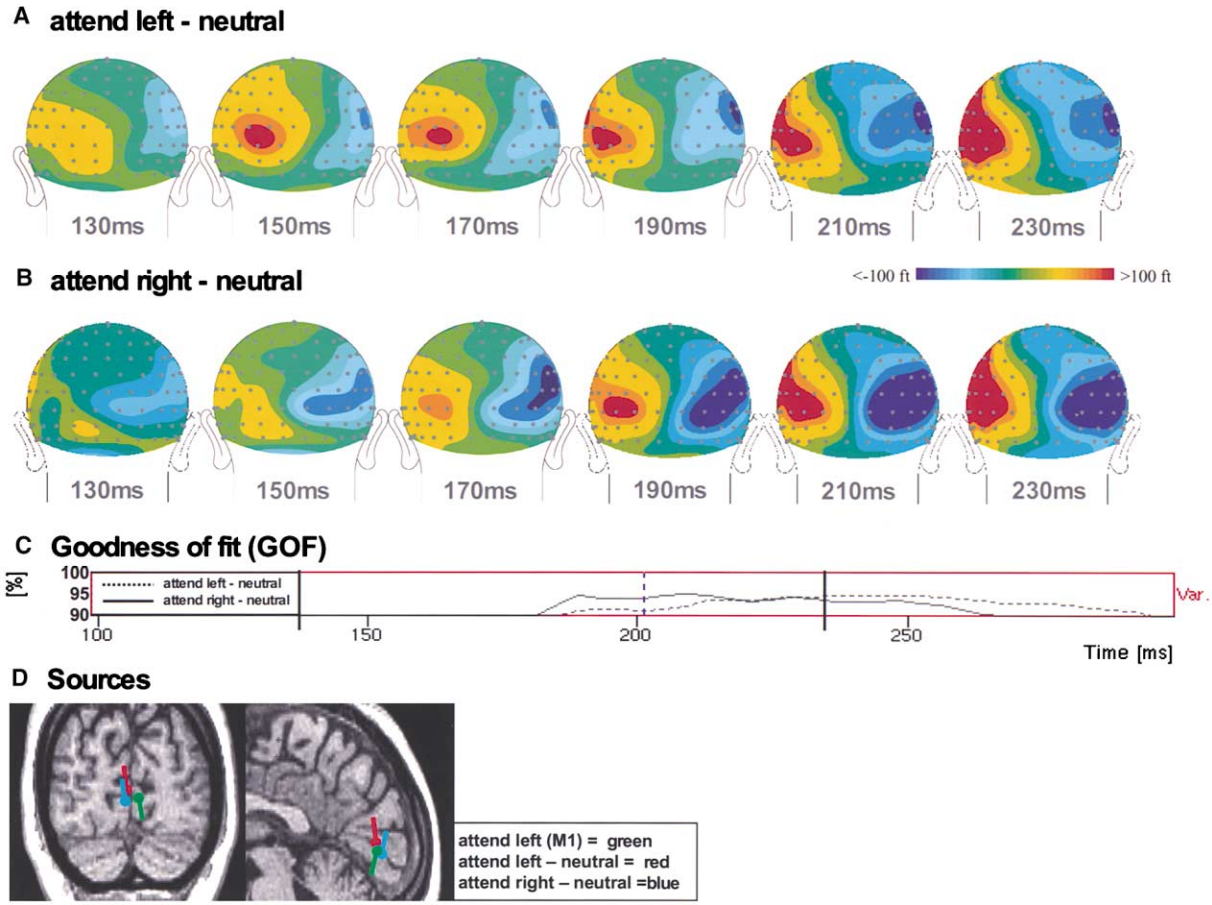

Figure 6. Time Course of the Late Attention Effect in Primary Visual Cortex

(A and B) Grand average ERMF distributions for the attend-left minus neutral and attend-right minus neutral differences at successive time intervals encompassing the late attention effect.

(C) Plot of GOF of the three-dipole model to these difference fields over time.

(D) Dipoles fit to the attend-left M1 component (75–91 ms) and to the attend-left minus neutral and attend-right minus neutral difference fields (calcarine dipoles at 189–224 ms) are projected onto anatomical MRI sections from a single subject.

that this late calcarine ERMF response reflects an enhanced processing of attended stimulus information in primary cortex in the time range 150–250 ms.

Further evidence that the late attention-related activity was generated in primary visual cortex was obtained by placing (seeding) dipoles at the loci of fMRI activations in the attend versus neutral contrasts. It was found that dipoles seeded to the V1 activations accounted for the late MEG attention effect better than dipoles seeded to either lingual or fusiform gyrus activations. An inverse modeling technique that uses a distributed source model (LORETA) also indicated a compact clustering of sources localized to calcarine cortex rather than being diffusely distributed. A further consideration is that the dipoles fit to the late attention effect in the attend versus neutral comparisons were invariably oriented superiorly and were approximately perpendicular to the calcarine fissure. Such an orientation is consistent with a neural generator in area V1 within the calcarine fissure but not in area V2, which is situated along the medial wall of the occipital lobe (Sereno et al., 1995) and hence would produce a dipolar source having a primarily horizontal orientation.

Previous studies have provided some evidence for long-latency activity in primary visual cortex in humans during spatial attention. Aine et al. (1995) presented ERMF recordings from a single subject showing an attention-related modulation of activity localized to the calcarine region at 130–160 ms. As in the present study, Aine et al. (1995) found that the dipole representing the delayed attention-related response in V1 was colocalized with the dipole that was fit to the earlier M1 response at around 90 ms but was opposite in polarity. This is consistent with the present data and suggests a mechanism whereby delayed feedback activates different cortical layers and/or different synaptic configurations than does the initial sensory input into area V1 (Mehta et al., 2000). In any case, the present MEG data, together with the converging fMRI evidence, provide strong support for the hypothesis that the primary visual cortex is reactivated in the 150–250 ms time range following a stimulus within the focus of spatial attention.

Martinez et al. (1999) also hypothesized a delayed feedback mechanism to account for their finding of an increased BOLD response in area V1 contralateral to the attended visual field while the initial evoked re-

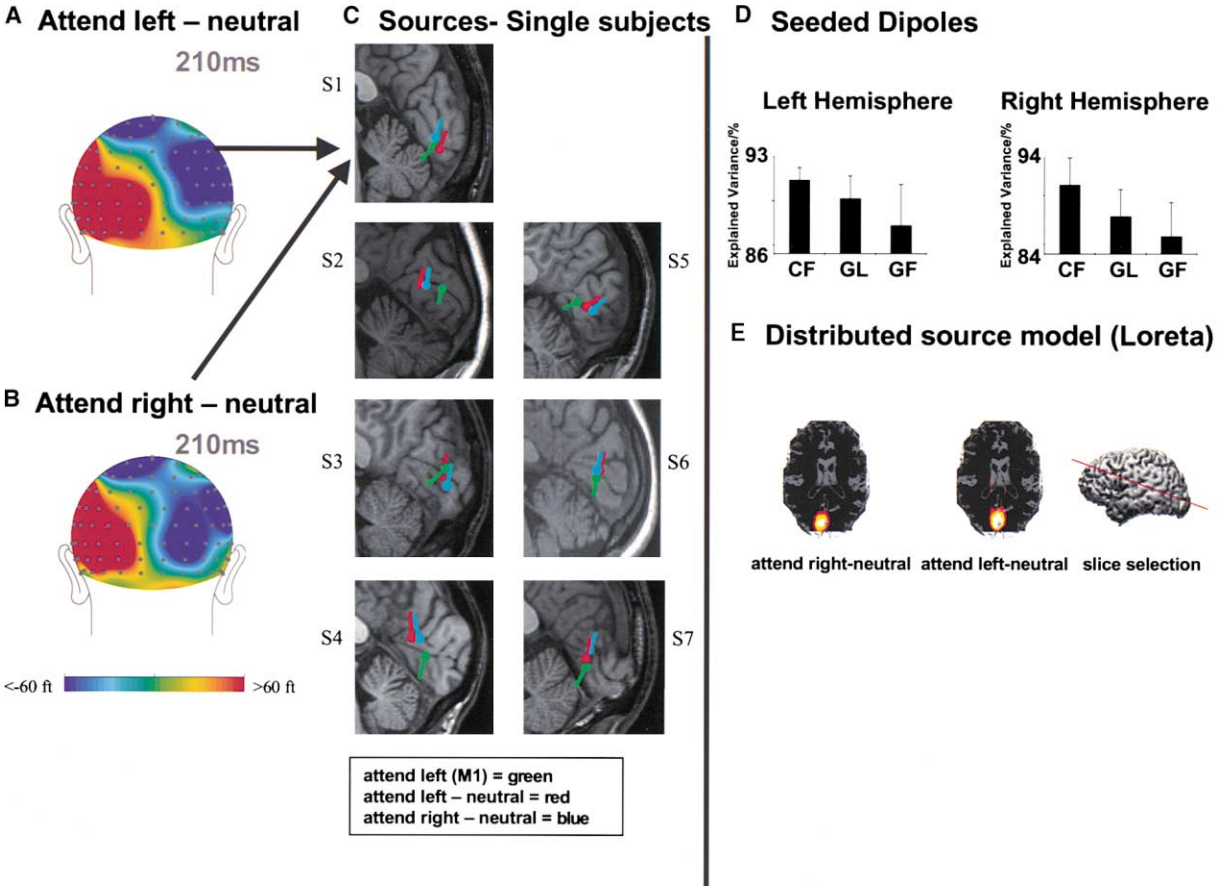

Figure 7. Late Attention Effect in Primary Visual Cortex in Individual Subjects

(A and B) ERMF distributions for attend-left minus neutral and attend-right minus neutral comparisons at 210 ms in an individual subject.

(C) Calcarine dipoles fit to attend-left minus neutral and attend-right minus neutral difference fields in the interval of the late attention effect (173–232 ms) in seven individual subjects, compared with dipoles fit to early M1 (75–91 ms).

(D) Percent of variance of late attention effect (averaged over six subjects) accounted for by dipoles seeded to the local maxima of measured BOLD modulations in calcarine, lingual, and fusiform areas (see Figure 3B).

(E) Distributed source model (LORETA) at 200–220 ms for the attend-right and attend-left versus neutral attention effects (grand average).

sponse (the C1 at 55–90 ms) in primary cortex remained invariant. Consistent with this hypothesis, dipole modeling of the ERP attention effects showed that the calcarine dipole fit to the early C1 also accounted for a late attention-related modulation in the 160–250 ms range (Martinez et al., 2001). This delayed attention effect was only evident in the source waveforms of the dipole model, however, and was not seen directly in the ERP waveforms, probably because it was overshadowed by concurrent activity arising from neighboring extrastriate areas. In contrast, in the present MEG recordings, the delayed attention effect localized to calcarine cortex could be observed directly, presumably because its dipolar source was oriented tangentially to the scalp and thus produced a stronger magnetic signal than the more radially oriented extrastriate generators. This delayed MEG effect (at 140–250 ms) was evident both in the attend-left versus attend-right and in the attend left/right versus neutral comparisons, and these same comparisons showed strong contralateral fMRI activation in area V1 in all subjects. This correspondence between the late MEG effect and the lateralized hemodynamic response strongly suggests that the long-latency attention effect observed here was associated with spatially selective attentional processing and not with nonselective aspects of task performance such as task difficulty.

The present findings together with those mentioned above suggest that the following sequence of cortical events unfolds during visual-spatial attention. The initial burst of neural activity triggered in area V1 at 55–60 ms does not seem to be affected by attention, and the earliest enhancement of attended inputs takes place in extrastriate areas (in or near areas V3/VP, V3a, and V4) beginning at 75–80 ms. These enhanced extrastriate signals, reflected in the enlarged P1 component at 80–130 ms, then influence processing in area V1 in the time range 140–250 ms, presumably by means of feedback connections to V1 from these higher extrastriate areas. An alternative mechanism, however, would be that the enhanced extrastriate signal is sent to another area specialized for attentional control that in turn projects to area V1 (Super et al., 2001). Whatever the exact mechanism, this delayed activity in area V1 might play an important role in enhancing the figure-ground contrast and

the salience of stimuli at attended locations (Lamme and Spekreijse, 2000; Super et al., 2001).

Experimental Procedures

Subjects

Nine healthy adult subjects (six male, age range 19–35 years, mean age = 25.7 years) with no psychiatric or neurological disorders participated in the MEG/ERP recordings after providing written informed consent. Of these subjects, six (four male, mean age = 26.2 years) also participated in the fMRI study, which used the same stimuli and task.

Stimuli and Tasks

During testing, subjects maintained fixation on a central cross while stimuli were presented on a projection screen adapted to either the MEG recording chamber or the fMRI scanner, respectively. The bilateral task stimuli consisted of a 3 × 3 array of "plus" signs in each visual field superimposed upon a background checkerboard that was both globally and locally smoothed (Figure 1). The central element in each array was a letter "T" that could be displayed either upright or inverted on a random 50/50 basis. Each trial block began with an attention-directing cue lasting 500 ms (either a left arrow, a right arrow, or a neutral cue indicated by a diamond), followed after an interval of either 500 ms (20%) or 3500 ms (80%) by a sequence of ten of the bilateral arrays. The bilateral arrays each lasted 200 ms and were separated by ISIs jittered randomly from 800–4000 ms (mean = 1000 ms, Poisson distribution). Each 3 × 3 array subtended 1.2° × 1.2° and was presented at an eccentricity of 6.0° (fixation point to center) with the lower edge 1.0° above the horizontal meridian (upper visual field stimulation). Each trial block lasted 18 s.

The subject's task on the blocks with the left or right arrow cues was to covertly direct attention to the arrays in the indicated visual field (ignoring the simultaneous array in the opposite field) and report by pressing one of two buttons whether the T at the center of each array was upright or inverted. Following the diamond ("neutral condition"), the task was simply to push a button upon the appearance of each bilateral array with no discrimination required. A hit was considered as a button press within 200–1000 ms after target delivery. Other responses were considered as false alarms. Subjects were given an initial training session and had to achieve 75% correct discriminations before continuing to the MEG/ERP recording session, which was followed by the fMRI session on a different day within the same week for six of the subjects. The discrimination task was difficult in that subjects only reached the above mentioned accuracy criterion after 0.5–2 hr of extensive training. The stimulus parameters (luminance, contrast, presentation time, eccentricity) were held constant across the ERP/MEG and fMRI sessions as well as across all subjects.

MR Data Acquisition

Subjects were scanned with a neuro-optimized GE Signa LX 1.5 T system (General Electric, Milwaukee, WI). In a structural session, whole-head T1 weighted images were acquired (quadrature head coil 3D-SPGR echo sequence, TR/TE/flip angle = 24 ms/8 ms/30°, spatial resolution 1 mm × 1 mm × 1.5 mm, matrix 256 × 256 × 124).

During task performance, functional data from 14 slices (5 in. surface coil, TR/TE/flip angle = 2000 ms/40 ms/80°, ramp sampling on, matrix 64 × 64, field of view 18 cm, slice thickness 3 mm, no gap, orientation perpendicular to the calcarine fissure) covering the occipital cortex were collected. The experiment consisted of eight runs, each lasting 580 s (290 volumes). During each run, eight blocks of each attention condition (left, right, neutral) and six blocks of an additional passive fixation condition were presented in a pseudorandom, counterbalanced order. In a separate session, fMRI data for determining individual field sign maps of the retinotopically organized visual areas were obtained using the method of Sereno et al. (1995), modified according to Tootell et al., (1997).

During functional runs, eye movements were controlled using a video recording system showing movements of the left eye by means of an infrared light transmission device. The resolution of this system for the detection of eye movements was better than 0.5°. Performance was monitored online, and all subjects were able to maintain fixation with <1° deviation.

fMRI Analysis

After standard preprocessing steps (slice-acquisition-time and motion correction, normalization, spatial smoothing, high and low-pass filtering, and rescaling to the global mean; SPM99, Wellcome Department of Cognitive Neurology, UK), the statistical analysis of the block design was performed using a box-car reference function convolved with a modeled hemodynamic response function and the temporal derivative of the box-car function for each subject (SPM99). Individual anatomical scans were coregistered with the functional images and normalized to 1 × 1 × 1 mm^3 to serve as an overlay for the activated areas.

In addition, for each subject, activated voxels of the contrast attend-right versus attend-left were identified and used as regions of interest for a subsequent analysis in which cue and stimulus-related modulations of the BOLD response could be separated using a deconvolution procedure (Burock and Dale, 2000; Hinrichs et al., 2000). Because of the wide jittering of ISIs in the experimental paradigm (see Adjar framework of Woldorff, 1993), an approach that is similar to that of adding randomized nonevents to the stimulus sequence (Burock et al., 1998), a deconvolution of the BOLD signal could be performed that allowed separate BOLD response curves to be calculated in response to the initial cue and to the subsequent task stimuli under the three task conditions (attend-right, attend-left, and neutral). These separated BOLD signals were analyzed for statistical significance by means of SPM99 and overlayed with the retinotopic field sign maps of each individual subject. The significance level for activations in individual subjects was set to $p < 0.05$ (corrected for multiple comparisons). Since a specific hypothesis for the primary visual area based on previous studies was given, the threshold for this region was set to $p < 0.05$, uncorrected. Contrast images from all six subjects were used to estimate the cue- and stimulus-related group effects using a random effects model (SPM99, Wellcome Department of Cognitive Neurology, UK). Group effects were thresholded at $p < 0.05$, corrected for cluster size (Poline et al., 1997).

MEG/EEG Recording

MEG data were recorded (sampling rate 255 Hz, bandwidth 0.0–50 Hz) using a 148 magnetometer whole head system (Magnes 2500 WH, 4-D-Neuroimaging). EEG data were acquired simultaneously from 32 electrode sites (Fp1, Fp2, F7, F3, Fz, F4, F8, FC1, FC2, T7, C3, Cz, C4, T8, CP1, CP2, P7, P3, Pz, P4, P8, PO7, PO3, PO4, PO8, Oz, O9, Iz, and O10, left mastoid, right horizontal, and vertical EOG according to the 10-20 system of the American Electroencephalographic Society) at the same sampling rate and bandwidth as the MEG. The MEG sensor coordinates were localized with respect to the subject's head using a spatial digitization device (Polhemus Fastrack). Coregistration of the MEG sensors with the individual structural MR images was accomplished by interactively localizing skull landmarks in the images. Eye movements were monitored in the same way as during fMRI.

ERMF/ERP Data Processing

After artifact rejection (peak-to-peak amplitude criterion of 100 μV), ERPs were selectively averaged for each attention condition (attend-left, attend-right, and neutral). ERP components were quantified as mean amplitudes over specified latency ranges with respect to a 200 ms prestimulus baseline.

Environmental noise was removed from the ERMF recordings by subtracting an individually weighted sum of MEG reference signals (picked up from eight additional sensors located ~20 cm distance from the helmet's surface) from each of the MEG channels (see Robinson, 1989). In a second step, artifacts were removed using a peak-to-peak amplitude criterion of 5 pT. ERMFs were separately averaged for each attention condition over a 1.0 s epoch with a 200 ms prestimulus baseline that was used as a reference interval for amplitude measures.

Individual subject's ERMFs were recalculated for a standardized grid of 164 virtual sensor positions using a method proposed by Ilmoniemi (1993) as implemented in the ASA program (A.N.T. Soft-

ware, Enschede, The Netherlands). From these standardized data, the grand average fields were derived.

In the occipital region, the ERP/ERMF grand average waveforms exhibited two main dipolar components in the attention-related waveforms, the first ranging from ~90 to 120 ms and the second from ~200 to 220 ms. The corresponding baseline-corrected ERP amplitude values were calculated for each individual subject data set over these latency ranges for the posterior electrodes covering the area where the attend-left versus attend-right difference (grand average) exhibited the strongest field power (see Figure 4)

For the ERMF waveforms, the corresponding baseline-corrected amplitude values were calculated for each individual subject as mean values over these latency ranges for four sensors covering the areas over the left and right hemisphere where the attend-left versus attend-right difference (grand average) exhibited the strongest field power (see Figure 5). Amplitude values from groups of sensors with locations symmetrical with respect to midline were subjected to a repeated analysis of variance with hemisphere and field of attention as within subject factors. The corresponding hemisphere x attention p values were separately derived for the early and late latency ranges.

For both individual and grand average ERP waveforms, equivalent current dipoles (ECD) were fit to the distributions of specific occipital components that were significant in the attend-right versus attend-left comparison, minimizing the average least square error between the forward solution and the observed data (CURRY 4.0, Neurosoft).

For the ERMFs, separate dipole models were derived over the same time intervals as for the ERPs for comparisons among the three attention conditions (attend-right versus attend-left, attend-right versus neutral, attend-left versus neutral). In addition, the sensory-evoked C1/M1 component was fit with a single ECD, both for the ERP and ERMF distributions. During fitting, the location and orientation of the model dipole sources were iteratively adjusted to minimize the error between the observed and forward solution fields.

The longer-latency attention effect required several dipoles to obtain an adequate fit. A single dipole in the medial occipital lobe generally provided the best fit at the latency of this effect. However, to meet our minimum criterion (for the grand average fields: 90% GOF across all channels used), two more dipoles needed to be added to the model, which were located in central and/or parietal regions. Thus, for individual subjects, the attend-right versus neutral and attend-left versus neutral differences were fit with a three ECD model. The strategy of dipole modeling for individual subjects followed the logic mentioned above. However, due to a lower signal-to-noise ratio, the minimal goodness of fit for individual subjects was set to 80%.

To further validate the localization of the ECD sources of the attend right/left versus neutral difference fields with an independent method, we calculated a distributed current source model based on the second order spatial derivatives of the current distribution (LORETA) (Pasqual-Marqui et al., 1994). This model provides an unbiased estimate of the location and distribution of possible sources that is relatively insensitive to depth normalization. The centers of calculated current distribution clusters reportedly provide more accurate estimations of deeper source activity than do other distributed source models (Fuchs et al., 1999). Accordingly, these models are well suited to be compared with calculated ECD solutions.

Acknowledgments

This work was supported by DFG Grant HE-1531/3-5, BMBF Grant 07-NBL 04/01ZZ9505TpA7, and NIMH Grant MH-25594. The authors are grateful to M. Scholz for technical support and J.M. Hopf for helpful discussions.

Received: November 27, 2001
Revised: May 6, 2002

References

Aine, C.J., Supek, S., and George, J.S. (1995). Temporal dynamics of visual-evoked neuromagnetic sources: effects of stimulus parameters and selective attention. Int. J. Neurosci. *80*, 79–104.

Aine, C.J., Supek, S., George, J.S., Ranken, D., Lewine, J., Sanders, J., Best, E., Tiee, W., Flynn, E.R., and Wood, C.C. (1996). Retinotopic organization of human visual cortex: departures from the classical model. Cereb. Cortex *6*, 354–361.

Brefczynski, J.A., and DeYoe, E.A. (1999). A physiological correlate of the 'spotlight' of visual attention. Nat. Neurosci. *2*, 370–374.

Burock, M.A., and Dale, A.M. (2000). Estimation and detection of event-related fMRI signals with temporally correlated noise: a statistically efficient and unbiased approach. Hum. Brain Mapp. *11*, 249–260.

Burock, M.A., Buckner, R.L., Woldorff, M.G., Rosen, B.R., and Dale, A.M. (1998). Randomized event-related experimental designs allow for extremely rapid presentation rates using functional MRI. Neuroreport *9*, 3735–3739.

Clark, V., and Hillyard, S.A. (1996). Spatial selective attention affects early extrastriate but not striate components of the visual evoked potential. J. Cogn. Neurosci. *8*, 387–402.

Clark, V.P., Fan, S., and Hillyard, S.A. (1995). Identification of early visual evoked potential generators by retinotopic and topographic analyses. Hum. Brain Mapp. *2*, 170–187.

Dale, A.M. (1999). Optimal experimental design for event-related fMRI. Hum. Brain Mapp. *8*, 109–114.

Desimone, R. (1998). Visual attention mediated by biased competition in extrastriate visual cortex. Philos. Trans. R. Soc. Lond. B Biol. Sci. *353*, 1245–1255.

DiRusso, F., Martinez, A., Sereno, M., Pitzalis, S., and Hillyard, S. (2002). The cortical sources of the early components of the visual evoked potential. Hum. Brain Mapp. *15*, 95–111.

Fuchs, M., Wagner, M., Kohler, T., and Wischmann, H.A. (1999). Linear and nonlinear current density reconstructions. J. Clin. Neurophysiol. *16*, 267–295.

Gandhi, S.P., Heeger, D.J., and Boynton, G.M. (1999). Spatial attention affects brain activity in human primary visual cortex. Proc. Natl. Acad. Sci. USA *96*, 3314–3319.

Gratton, G. (1997). Attention and probability effects in the human occipital cortex: an optical imaging study. Neuroreport *8*, 1749–1753.

Heinze, H.J., Luck, S.J., Mangun, G.R., and Hillyard, S.A. (1990). Visual event-related potentials index focused attention within bilateral stimulus arrays. I. Evidence for early selection. Electroencephalogr. Clin. Neurophysiol. *75*, 511–527.

Heinze H.J., Mangun G.R., Burchert W., Hinrichs H., Scholz M., Munte T.F., Gos A., Scherg M., Johannes S., Hundeshagen H., et al. (1994). Combined spatial and temporal imaging of brain activity during visual selective attention in humans. Nature *372*, 543–546.

Hillyard, S.A., and Anllo-Vento, L. (1998). Event-related brain potentials in the study of visual selective attention. Proc. Natl. Acad. Sci. USA *95*, 781–787.

Hinrichs, H., Scholz, M., Tempelmann, C., Woldorff, M.G., Dale, A.M., and Heinze, H.J. (2000). Deconvolution of event-related fMRI responses in fast-rate experimental designs. Tracking amplitude variations. J. Cogn. Neurosci. *12*, 76–89.

Ilmoniemi, R.J. (1993). Models of source currents in the brain. Brain Topogr. *5*, 331–336.

Ito, M., and Gilbert, C.D. (1999). Attention modulates contextual influences in the primary visual cortex of alert monkeys. Neuron *22*, 593–604.

Josephs, O., and Henson, R.N. (1999). Event-related functional magnetic resonance imaging: modelling, inference and optimization. Philos. Trans. R. Soc. Lond. B Biol. Sci. *354*, 1215–1228.

Kastner, S., Pinsk, M.A., De Weerd, P., Desimone, R., and Ungerleider, L.G. (1999). Increased activity in human visual cortex during directed attention in the absence of visual stimulation. Neuron *22*, 751–761.

Lamme, V.A., and Spekreijse, H. (2000). Contextual modulation of primary visual cortex activity representing attentive and conscious scene perception. In The New Cognitive Neurosciences, M.S. Gazzaniga, ed. (Cambridge, MA: MIT Press), pp. 279–290.

Lange, J.J., Wijers, A.A., Mulder, L.J., and Mulder, G. (1998). Color

selection and location selection in ERPs: differences, similarities and 'neural specificity'. Biol. Psychol. *48*, 153–182.

Luck, S.J., Heinze, H.J., Mangun, G.R., and Hillyard, S.A. (1990). Visual event-related potentials index focused attention within bilateral stimulus arrays. II. Functional dissociation of P1 and N1 components. Electroencephalogr. Clin. Neurophysiol. *75*, 528–542.

Luck, S.J., Chelazzi, L., Hillyard, S.A., and Desimone, R. (1997). Neural mechanisms of spatial selective attention in areas V1, V2, and V4 of macaque visual cortex. J. Neurophysiol. *77*, 24–42.

Mangun, G.R., Hopfinger, J., Kussmaul, C., Fletcher, E., and Heinze, H.J. (1997). Covariations in PET and ERP measures of spatial selective attention in human extrastriate visual cortex. Hum. Brain Mapp. *5*, 273–279.

Martinez, A., Anllo-Vento, L., Sereno, M.I., Frank, L.R., Buxton, R.B., Dubowitz, D.J., Wong, E.C., Hinrichs, H., Heinze, H.J., and Hillyard, S.A. (1999). Involvement of striate and extrastriate visual cortical areas in spatial attention. Nat. Neurosci. *2*, 364–369.

Martinez, A., DiRusso, F., Anllo-Vento, L., Sereno, M.I., Buxton, R.B., and Hillyard, S.A. (2001). Putting spatial attention on the map: timing and localization of stimulus selection processes in striate and extrastriate visual areas. Vision Res. *41*, 1437–1457.

Maunsell, J.H., and McAdams, C.J. (2000). Effects of attention on neuronal response properties in visual cerebral cortex. In The New Cognitive Neurosciences, M.S. Gazzaniga, ed. (Cambridge, MA: MIT Press), pp. 315–324.

McAdams, C.J., and Maunsell, J.H. (1999). Effects of attention on orientation-tuning functions of single neurons in macaque cortical area V4. J. Neurosci. *19*, 431–441.

Mehta, A.D., Ulbert, I., and Schroeder, C.E. (2000). Intermodal selective attention in monkeys. I. distribution and timing of effects across visual areas. Cereb. Cortex *10*, 343–358.

Motter, B.C. (1993). Focal attention produces spatially selective processing in visual cortical areas V1, V2, and V4 in the presence of competing stimuli. J. Neurophysiol. *70*, 909–919.

Pasqual-Marqui, R.D., Michel, C.M., and Lehmann, D. (1994). Low resolution electromagnetic activity in the brain. Int. J. Psychophysiol. *18*, 49–65.

Poline, J.B., Worsley, K.J., Evans, A.C., and Friston, K.J. (1997). Combining spatial extent and peak intensity to test for activations in functional imaging. Neuroimage *5*, 83–96.

Posner, M.I., and Gilbert, C.D. (1999). Attention and primary visual cortex. Proc. Natl. Acad. Sci. USA *96*, 2585–2587.

Ress, D., Backus, B.T., and Heeger, D.J. (2000). Activity in primary visual cortex predicts performance in a visual detection task. Nat. Neurosci. *3*, 940–945.

Robinson, S.E. (1989). Environmental noise cancellation for biomagnetic measurements. In Advances in Biomagnetism, S.J. Williamsen, and M. Hoke, eds. (New York: Plenum Press), pp. 721–724.

Roelfsema, P.R., Lamme, V.A., and Spekreijse, H. (1998). Object-based attention in the primary visual cortex of the macaque monkey. Nature *395*, 376–381.

Sengpiel, F., and Huebener, M. (1999). Visual attention: spotlight on the primary visual cortex. Curr. Biol. *9*, 318–321.

Sereno, M.I., Dale, A.M., Reppas, J.B., Kwong, K.K., Belliveau, J.W., Brady, T.J., Rosen, B.R., and Tootell, R.B. (1995). Borders of multiple visual areas in humans revealed by functional magnetic resonance imaging. Science *268*, 889–893.

Somers, D.C., Dale, A.M., Seiffert, A.E., and Tootell, R.B. (1999). Functional MRI reveals spatially specific attentional modulation in human primary visual cortex. Proc. Natl. Acad. Sci. USA *96*, 1663–1668.

Super, H., Spekreijse, H., and Lamme, V.A.F. (2001). Two distinct modes of sensory processing observed in monkey primary visual cortex (V1). Nat. Neurosci. *4*, 304–310.

Tootell, R.B., Mendola, J.D., Hadjikhani, N.K., Ledden, P.J., Liu, A.K., Reppas, J.B., Sereno, M.I., and Dale, A.M. (1997). Functional analysis of V3A and related areas in human visual cortex. J. Neurosci. *17*, 7060–7078.

Tootell, R.B., Hadjikhani, N., Hall, E.K., Marrett, S., Vanduffel, W., Vaughan, J.T., and Dale, A.M. (1998). The retinotopy of visual spatial attention. Neuron *21*, 1409–1422.

Vidyasagar, T.R. (1998). Gating of neuronal responses in macaque primary visual cortex by an attentional spotlight. Neuroreport *9*, 1947–1952.

Vidyasagar, T.R. (1999). A neuronal model of attentional spotlight: parietal guiding the temporal. Brain Res. Brain Res. Rev. *30*, 66–76.

Wijers, A.A., Lange, J.J., Mulder, G., and Mulder, L.J. (1997). An ERP study of visual spatial attention and letter target detection for isoluminant and nonisoluminant stimuli. Psychophysiology *34*, 553–565.

Woldorff, M.G. (1993). Distortion of ERP averages due to overlap from temporally adjacent ERPs: analysis and correction. Psychophysiology *30*, 98–119.

Woldorff, M.G., Fox, P.T., Matzke, M., Lancaster, I.L., Veeraswamy, S., Zamarripa, F., Seaboldt, M., Glass, T., Gao, J.H., Martin, C.C., and Jerabek, P. (1997). Retinotopic organization of early visual spatial attention effects as revealed by PET and ERPs. Hum. Brain Mapp. *5*, 280–286.